

## Enhancement of photocatalytic properties of TiO<sub>2</sub> for NO photo-oxidation by optimized sol–gel synthesis

E. Luévano-Hipólito<sup>1</sup> · A. Martínez de la Cruz<sup>1</sup>

Received: 8 February 2016 / Accepted: 12 March 2016 / Published online: 28 March 2016  
© Springer Science+Business Media Dordrecht 2016

**Abstract** TiO<sub>2</sub> samples were prepared by the sol–gel method applying a factorial design in order to improve the photocatalytic properties of the semiconductor oxide for the nitric oxide (NO) photo-oxidation reaction. The temperature of calcination and the amount of alcohol and acid used in the course of the sol–gel reaction were selected as critical experimental variables. As the products of the factorial design, 27 TiO<sub>2</sub> samples were obtained and characterized by X-ray powder diffraction, scanning electron microscopy, transmission electron microscopy, diffuse reflectance spectroscopy, and adsorption–desorption N<sub>2</sub> isotherms. The photocatalytic activity of the TiO<sub>2</sub> samples was evaluated in the NO photo-oxidation reaction under UV irradiation. The conversion degree of NO reached by each sample was associated with its physicochemical properties, finding a stronger dependence with the temperature of calcination and morphology of the samples. Different photocatalytic reaction parameters were modified such as mass of photocatalyst, irradiance, flow rate of gas, and relative humidity in order to evaluate their effect in the constants of velocity and adsorption. The TiO<sub>2</sub> sample with the highest photocatalytic activity was exposed under different experimental conditions to evaluate its selectivity for the formation of innocuous nitrate ions as final product of the NO photo-oxidation reaction.

**Keywords** Heterogeneous photocatalysis · TiO<sub>2</sub> · NO<sub>x</sub> · Air pollution

---

✉ A. Martínez de la Cruz  
aazael70@yahoo.com.mx

<sup>1</sup> CIIDIT, Facultad de Ingeniería Mecánica y Eléctrica, Universidad Autónoma de Nuevo León, Ciudad Universitaria, C.P. 66451 San Nicolás de los Garza, NL, Mexico

## Introduction

The nitrogen oxides commonly identified as  $\text{NO}_x$  are a group of highly reactive gases, all of which contain nitrogen and oxygen in varying stoichiometric amounts. In these compounds, the nitrogen appears in a wide variety of oxidation states, from 4+ ( $\text{NO}_2$ ), 2+ ( $\text{NO}$ ) to 1+ ( $\text{N}_2\text{O}$ ). However, the nitrogen oxides emissions subject to governmental regulations are uniquely nitric oxide ( $\text{NO}$ ) and nitrogen dioxide ( $\text{NO}_2$ ) which together are referred as  $\text{NO}_x$  [1, 2]. These emissions are formed by the oxidation of the nitrogen present in fuels at high temperatures and their main sources are combustion engine vehicles followed by electric utilities and industrial activity.  $\text{NO}_x$  gases have a negative impact in the environment, for human and animal health as well as in vegetation [3, 4]. For example, these pollutants are involved in the formation of tropospheric ozone, the precursor of serious respiratory problems. Furthermore, in combination with other atmospheric components, they produce acid rain, causing acidification of rivers and lakes and the corrosion of buildings. In general,  $\text{NO}$  gas represents 95 % of all nitrogen oxide emissions. From a thermodynamically point of view, this compound is unstable but the decomposition reaction is inhibited due to its high activation energy ( $365 \text{ kJ mol}^{-1}$ ) [5]. In contrast, the oxidation of  $\text{NO}$  to  $\text{NO}_2$  is a thermodynamically favored process which takes place at ambient conditions (1 bar,  $25^\circ\text{C}$ ). In this sense, the heterogeneous photocatalysis is an innovative and promising technique to promote the photo-oxidation reaction of  $\text{NO}_x$  to innocuous  $\text{NO}_3^-$  ions [6–11].

Titanium dioxide ( $\text{TiO}_2$ ) has been widely used as a photocatalyst due to its redox ability, chemical stability and non-toxicity [12]. In particular, the commercial oxide  $\text{TiO}_2$  (Degussa, P-25) has shown a good performance in the  $\text{NO}_x$  photo-oxidation reaction reaching conversion degrees in the range of 35–90 %. These values of  $\text{NO}$  conversion degrees were enhanced mainly by modifying the operating conditions in the photocatalytic reactor [13–17], paying little attention to physicochemical properties developed by the semiconductor oxide in an optimized synthesis. The sol–gel synthesis provides the formation of  $\text{TiO}_2$  synthetic with a high specific surface area, low crystallite size, and anatase and rutile content balance [18]. In the past,  $\text{TiO}_2$  obtained by the sol–gel method was used successfully as a photocatalyst in aqueous media.

In the present work, the synthesis of  $\text{TiO}_2$  was carried out by sol–gel modifying some experimental conditions (temperature, and amount of alcohol and acid) in order to check their effects in the physicochemical properties of the material, and consequently in its photocatalytic activity. The samples were tested as photocatalysts in the  $\text{NO}$  photo-oxidation reaction, and their activities were associated with the physicochemical properties developed during the sol–gel synthesis. Beyond the assessment of the photocatalytic activity of  $\text{TiO}_2$  samples for the photo-oxidation of  $\text{NO}$ , the selectivity of the  $\text{TiO}_2$  to produce innocuous  $\text{NO}_3^-$  ions as final products of reaction has been revised.

## Experimental

### Synthesis of TiO<sub>2</sub>

TiO<sub>2</sub> samples were synthesized by the sol–gel method applying a factorial design of the type 3<sup>n</sup> ( $n = 3$ ) to study the effect of three experimental conditions on the final physicochemical properties of TiO<sub>2</sub>. In a typical experiment, titanium isopropoxide {Ti[OCH(CH<sub>3</sub>)<sub>2</sub>]<sub>4</sub>} TTIP (Aldrich, 97 %) was diluted in different amounts of ethyl alcohol (CH<sub>3</sub>CH<sub>2</sub>OH) (DEQ, 99 %) to obtain molar ratios of 1:17, 1:34, and 1:51. The mixture was homogenized with continuous stirring for 30 min to promote the formation of a sol, and then an acetic acid solution (CH<sub>3</sub>COOH) (J.T. Baker, 99 %) was added to start the hydrolysis and condensation reactions. The volume of acetic acid added to the medium was 5, 10, and 15 mL in each case. The resulting gel was maintained under vigorous stirring for 1 h and then aged for 1 day at room temperature. The gel obtained was dried at 100 °C for 24 h to promote the evaporation of the solvent until the formation of a beige powder. This material, identified hereafter as the precursor of TiO<sub>2</sub>, was heated in air at 300, 400, and 500 °C for 24 h to remove reaction by-products and promote the formation of the crystalline anatase polymorph of TiO<sub>2</sub>. For the factorial design was used the software Minitab™, which provides a randomized order to make the synthesis of 27 samples derived from the 3<sup>n</sup> design.

### Characterization

The structural characterization of TiO<sub>2</sub> samples was carried out by X-ray powder diffraction using a Bruker D8 Advance diffractometer with Cu K<sub>α</sub> radiation (40 kV, 30 mA). A typical run was made with a 0.05° step size and a dwell time of 0.5 s. To estimate the crystal size of the TiO<sub>2</sub> samples, the half-width of the strongest line in the diffraction patterns was followed. Taking these data, the crystal size of particles was calculated using the Scherrer equation. The morphology of the samples was analyzed by scanning electron microscopy and transmission electron microscopy using a FEI Nova NanoSEM 200 and a FEI Titan G2 80-300 microscopes with accelerating voltages of 30 and 300 kV, respectively. The UV–Vis diffuse reflectance absorption spectra of the samples were obtained using an Agilent Technologies UV–Vis-NIR spectrophotometer model Cary 5000 series equipped with an integrating sphere. The BET surface area measurements were carried out by adsorption–desorption N<sub>2</sub> isotherms by means of a Bel-Japan Minisorp II surface area and pore size analyzer. The isotherms were evaluated at –196 °C after pretreatment of the samples at 100 °C for 24 h.

### Photocatalytic experiments

The photocatalytic activity of TiO<sub>2</sub> samples was tested in the NO photo-oxidation reaction under UV irradiation, using a continuous flow reactor designed according with the ISO 22197-1. Table 1 shows the main operating conditions of the system

**Table 1** Experimental operating conditions in the photocatalytic reactor

Description	Operating conditions
Reactor	
Area (m <sup>2</sup> )	0.08
Light source	
Maximum emission wavelength UV (nm)	365
Flow rate (L min <sup>-1</sup> )	0.5–1.0
Irradiance flux (W m <sup>-2</sup> )	8.2–10.1
Relative humidity (%)	<0.4 ppm–70
NO inlet concentration (ppm)	0.6–1.5

employed in the photocatalytic experiments. The photocatalytic reactor was made of stainless steel with a volume of 0.8 L and was equipped with an integrated window in its superior part to allow the passage of UV radiation. The photocatalyst was coated over an area of 0.08 m<sup>2</sup> of a glass substrate by brush-coating a dispersion of the photocatalyst in ethanol. As inlet gas was used 3 ppm of NO mixture stabilized in N<sub>2</sub>. The concentration of inlet gas was adjusted to 1 ppm in NO by using synthetic air (20.5 vol% O<sub>2</sub> and 79.5 vol% N<sub>2</sub>) and the flow rate of gas was adjusted to 1 L min<sup>-1</sup>. The source of light irradiation consisted of two fluorescent black lamps (TecnoLite) of 20 W each, emitting mainly between 365 and 400 nm. The UV intensity in the center of the photocatalytic reactor measured by a digital radiometer CR10 (Q-Lab) was 8.2 W m<sup>-2</sup>. The concentration of NO was continuously measured with a chemiluminescent NO analyzer (EcoPhysics CLD88p) with a sampling rate of 0.5 L min<sup>-1</sup>. The amount of nitrate and nitrite ions produced was followed by the analysis of 50 mL of deionized water used in the wash of the photocatalyst after the photocatalytic reaction. For this purpose, powders of the photocatalyst used were sonicated in water for 30 min in order to desorb nitrates and nitrites, and then was centrifuged to obtain a crystalline solution. The concentration of nitrates and nitrites ions in solution was measured in a Hach colorimeter through the reduction of nitrate to nitrite using cadmium as a catalyst and by the diazotization method, respectively.

## Results and discussion

### Characterization

TiO<sub>2</sub> samples synthesized by the sol–gel method were characterized structurally by the X-ray powder diffraction technique. All diffraction lines were in agreement with the corresponding lines of the TiO<sub>2</sub> anatase polymorph according with the database JCPDS Card No. 21-1272, indicating that the samples were obtained in pure form at the level of resolution of X-ray diffraction. From the analysis of the XRD patterns, a difference in the crystallinity of the samples was observed which was related with its crystal size. The crystal size values of the TiO<sub>2</sub> samples ranged from 20 to 69 nm

(see Table 2). According to the profile of the XRD patterns, high calcination temperatures (500 °C) promoted the growth of TiO<sub>2</sub> crystals probably due to a particle coalescence that took place during the sintering process.

Diffuse reflectance spectra of TiO<sub>2</sub> samples were analyzed by UV–Vis spectroscopy in the range of 200–800 nm. All samples absorbed below 400 nm, indicating that the activation is given by the absorption of UV radiation of the electromagnetic spectrum. Based on the absorption spectra of the prepared TiO<sub>2</sub> samples, a UV lamp was chosen for the photocatalytic experiments. The radiation absorption by the semiconductor oxide is essential to start the photocatalytic process

**Table 2** Physicochemical properties of TiO<sub>2</sub> samples prepared by the sol–gel method

Experiments	Alcohol (mL)	Acid (mL)	T (°C)	Crystal size (nm)	Band gap (eV)	Surface area (m <sup>2</sup> g <sup>-1</sup> )
TiO <sub>2</sub> -1	10	10	500	29	3.20	67
TiO <sub>2</sub> -2	10	5	500	39	3.19	48
TiO <sub>2</sub> -3	30	5	400	22	3.20	106
TiO <sub>2</sub> -4	30	10	400	24	3.19	105
TiO <sub>2</sub> -5	10	10	400	23	3.20	104
TiO <sub>2</sub> -6	30	10	300	23	3.19	104
TiO <sub>2</sub> -7	20	10	300	23	3.18	107
TiO <sub>2</sub> -8	20	5	300	21	3.21	160
TiO <sub>2</sub> -9	30	20	300	22	3.20	111
TiO <sub>2</sub> -10	30	20	500	35	3.17	48
TiO <sub>2</sub> -11	30	20	400	24	3.22	102
TiO <sub>2</sub> -12	20	10	500	29	3.20	72
TiO <sub>2</sub> -13	20	10	400	24	3.20	96
TiO <sub>2</sub> -14	30	5	300	22	3.21	113
TiO <sub>2</sub> -15	20	20	400	24	3.19	87
TiO <sub>2</sub> -16	10	20	400	24	3.18	92
TiO <sub>2</sub> -17	10	5	400	25	3.17	91
TiO <sub>2</sub> -18	20	20	500	61	3.15	13
TiO <sub>2</sub> -19	10	20	500	69	3.19	151
TiO <sub>2</sub> -20	20	5	500	33	3.19	65
TiO <sub>2</sub> -21	10	5	300	22	3.21	117
TiO <sub>2</sub> -22	20	5	400	29	3.18	78
TiO <sub>2</sub> -23	30	10	500	36	3.16	57
TiO <sub>2</sub> -24	30	5	500	35	3.16	61
TiO <sub>2</sub> -25	20	20	300	21	3.18	121
TiO <sub>2</sub> -26	10	20	300	20	3.18	122
TiO <sub>2</sub> -27	10	10	300	20	3.23	122
TiO <sub>2</sub> P-25	–	–	–	35	3.10	50

because it provides the energy for the generation of the electron–hole pair. In this sense, the TiO<sub>2</sub> samples showed differences in the amount of radiation absorbed. In general, the samples calcined at low temperature (300 °C) had the highest absorption probably due to their crystal size. The energy band gap value of the TiO<sub>2</sub> samples was obtained using the Kubelka–Munk function and the results are listed in Table 2. The energy band gap values were from 3.15 to 3.23 eV and are consistent with those reported in the literature [19–21].

Adsorption–desorption N<sub>2</sub> isotherms of TiO<sub>2</sub> samples showed the typical behavior of mesoporous materials. The isotherms obtained were categorized as type IV with a hysteresis loop observed in the range of 0.7–1.0 P/P<sub>0</sub>, as is characteristic for materials with mesoporosity and a high energy of adsorption [22]. The specific surface area values are summarized in Table 2. In general, the surface area was affected by the calcination temperature, showing higher values at lower calcination temperatures (300 °C). In this regard, the samples calcined at 300 °C reached surface area values >100 m<sup>2</sup> g<sup>-1</sup>. The negative effect of increasing the calcination temperature on the surface area was associated with the growth of particles derived from the interaction between them.

The morphology of TiO<sub>2</sub> samples was investigated by scanning electron microscopy (SEM). In general, TiO<sub>2</sub> samples developed a heterogeneous morphology in the form of irregular spheres with different diameters. As a characteristic of the samples, they showed a high degree of agglomeration of primary particles.

### Photocatalytic activity

The photocatalytic activity of TiO<sub>2</sub> samples synthesized according to the factorial design was evaluated in the photo-oxidation reaction of nitric oxide under different experimental conditions. A typical experiment was performed at 25 °C with an initial NO concentration of 1 ppm, and a content of H<sub>2</sub>O vapor <0.4 ppm. Figure 1 shows the degree of NO conversion (%) reached after 2 h of UV irradiation, using as photocatalyst (50 mg) the 27 TiO<sub>2</sub> samples obtained from the factorial design. For all cases, the stationary state was reached in at least 30 min. A strong influence of the experimental conditions of synthesis over the degree of NO conversion was observed due to the physical properties developed in each TiO<sub>2</sub> sample. As an indication of the importance of the experimental conditions of synthesis in the degree of NO conversion, it was observed that these values ranged from 80 % (TiO<sub>2</sub>-7) to 11.3 % (TiO<sub>2</sub>-23). An additional experiment was performed in the absence of the photocatalyst in order to check the stability of the NO mixture when flowing throughout the system. This experiment revealed a null variation in the concentration of NO, confirming that the combination of photocatalyst + lamp irradiation was necessary to produce an appreciable reduction in the concentration of NO.

Figure 2 shows the profile of the evolution of the NO conversion degree from the beginning of the photocatalytic reaction to the system reaching the stationary state for the samples with the highest (TiO<sub>2</sub>-7) and lowest photocatalytic activity (TiO<sub>2</sub>-23). In the initial stage of the reaction, the sample TiO<sub>2</sub>-23 had a higher degree of NO conversion than the observed for the sample TiO<sub>2</sub>-7, which denoted a faster

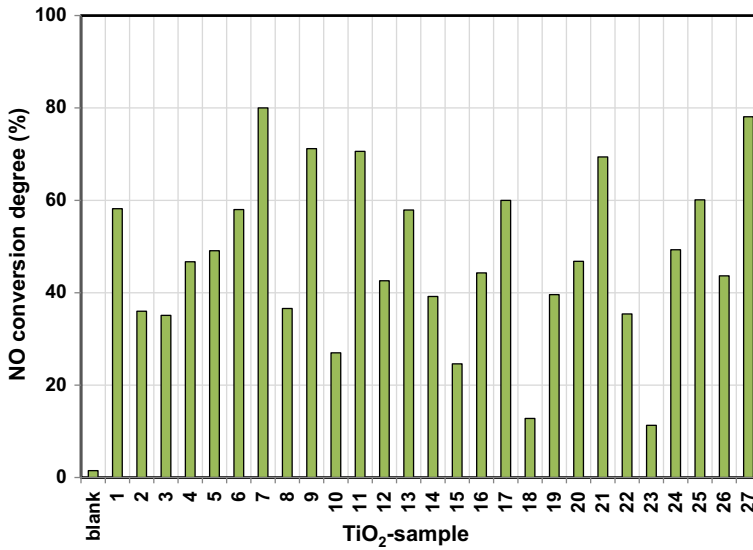


**Fig. 1** Degree of NO conversion (%) employing 50 mg of different TiO<sub>2</sub> photocatalysts after 2 h of UV irradiation ( $Q = 1 \text{ L min}^{-1}$ ,  $I = 8.2 \text{ W m}^{-2}$ )

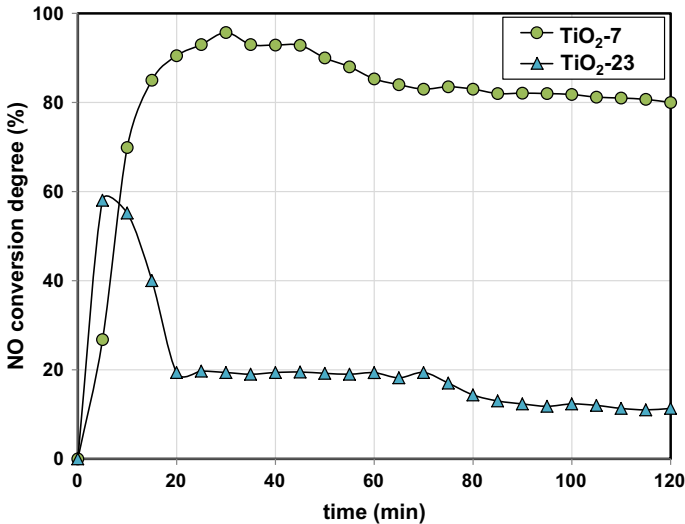


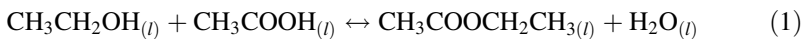
**Fig. 2** Evolution of the degree of NO conversion (%) using the samples TiO<sub>2</sub>-7 and TiO<sub>2</sub>-23 as photocatalysts ( $Q = 1 \text{ L min}^{-1}$ ,  $I = 8.2 \text{ W m}^{-2}$ )

activation process. However, after reaching a maximum degree of NO conversion of 60 %, the activity of the sample TiO<sub>2</sub>-23 fell markedly after 20 min of reaction reaching an apparent steady state around an 11 % degree of NO conversion during 2 h of UV irradiation. The activation of the sample TiO<sub>2</sub>-7 was more gradual

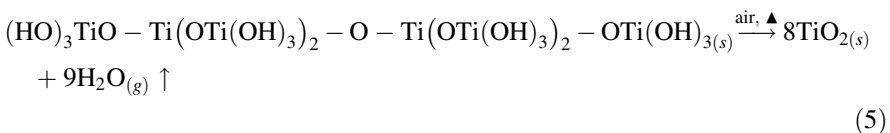
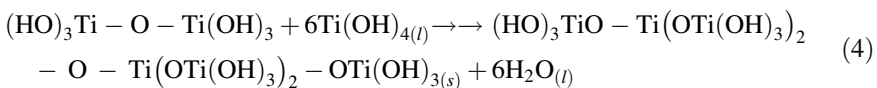
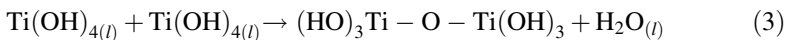
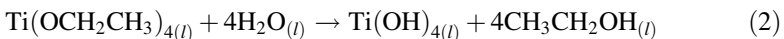
reaching a maximum degree of conversion of 95 % after 30 min and then decreasing to a value close to 80 % after 2 h of UV irradiation. The difference between the two photocatalytic activities may be associated with several factors, but given the amount of sample used in both experiments (50 mg in 0.08 m<sup>2</sup>), the adsorption was an important factor in the degree of NO conversion. In this sense, the adsorption of more NO molecules was favored in the sample TiO<sub>2</sub>-7, which has the double the specific surface area compared with the sample TiO<sub>2</sub>-23.

### Analysis of the factorial design

Once the structural, morphological, textural and optical characterization of the TiO<sub>2</sub> samples had been carried out, the corresponding values obtained were analyzed using the software Minitab. The allocation of magnitude of the impact of experimental conditions in the physicochemical properties of TiO<sub>2</sub> was performed using a Pareto chart with a confidence interval of 95 %. According to the results, temperature was the factor that had more influence on the physicochemical properties of the TiO<sub>2</sub> samples. The contribution of temperature to the physicochemical properties of oxide was associated with the sintering process that occurs in the particles during the heat treatment, which affects the crystallite size and specific surface area of the samples. Additionally, the amount of acid had a significant influence on the surface area developed by the samples. This fact may be related to the generation of H<sub>2</sub>O molecules by the esterification reaction of acetic acid and ethanol (Eq. 1).



The H<sub>2</sub>O molecules formed are available to participate in the hydrolysis reaction and thus promote TiO<sub>2</sub> precursors with high branching (Eqs. 2–5) [23].



Additionally, a Pareto chart was performed in order to corroborate from a statistical standpoint the effect of the experimental conditions of synthesis on the degree of NO conversion. As was expected, the most influential variable in the conversion degree of NO was the temperature. This is understandable because the



influence of temperature on the physicochemical properties such as surface area and crystallite size, which directly impact on the photocatalytic activity of the oxide.

Based on the obtained results, the software provided a mathematical model considering the degree of NO conversion as response (Eq. 6).

$$\text{Conversion (\%)} = 194.5 - 6.64A - 9.22B - 0.28C + 0.602AB + 0.01254AC + 0.0172BC - 0.001242ABC \quad (6)$$

where A represents the volume of alcohol (mL), B is the volume of acid (mL), and C corresponds to the calcination temperature (°C). Each coefficient estimates its effect on the degree of NO conversion by modifying the variables A, B or C when all other variables are constants. Also, the sign of each coefficient indicates the direction of the relationship. For example, by increasing the C variable (temperature), the degree of NO conversion decreases according to its negative sign. Considering the mathematical model (Eq. 6), the software determined, as optimal values of synthesis the conditions,  $A = 30$  mL,  $B = 20$  mL, and  $C = 300$  °C (TiO<sub>2</sub>-9) to obtain the best photocatalyst. However, when this experimental values combination was used, the degree of NO conversion reached was 71.2 %, i.e., 12 % less than the value predicted by the mathematical model. Although a good tendency was observed between the experimental and calculated values of the degree of NO conversion, Fig. 3 shows the existence of certain deviations in the comparison of both values. In general, an average error of 28 % was estimated. The origin of this deviation can be associated with some theoretical and experimental aspects. In the first instance, the model was calculated assuming a lineal regression, but the experimental data do not correspond entirely with a process with linear characteristics. In addition, there is an experimental error associated with the dispersion degree of the photocatalysts on the glass substrate. In this sense, the sample with the

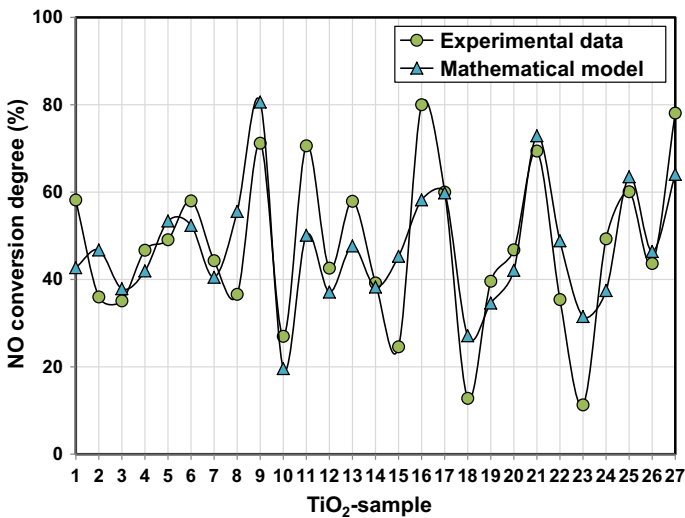


**Fig. 3** Comparison of NO conversion values (%) obtained from experimental data and using Eq. (6) when TiO<sub>2</sub> was employed as photocatalyst

highest surface area ( $\text{TiO}_2$ -8) does not have a good dispersion in the ethanol slurry and exhibited a relatively low activity. On the other hand, the model does not consider differences in the absorption degree of radiation by  $\text{TiO}_2$  samples, nor the differentiating factor of the preferential orientation of the crystalline planes of the  $\text{TiO}_2$  particles. In particular, the last factor was investigated in detail.

As was described earlier, SEM images of the different samples showed a similar morphology, and a differential factor between the 27 samples was not observed. For this reason, a deep analysis of the morphology of the samples was carried out by the TEM technique. For this purpose, the samples with the highest ( $\text{TiO}_2$ -7 and  $\text{TiO}_2$ -27) and lowest ( $\text{TiO}_2$ -18 and  $\text{TiO}_2$ -23) photocatalytic activity were selected. Figure 4a, b shows that the morphology of the samples  $\text{TiO}_2$ -7 and  $\text{TiO}_2$ -27 is characterized by semispherical particles with an average diameter of 10 and 15 nm, respectively. These values are similar to those calculated by X-ray diffraction. On the other hand, the samples  $\text{TiO}_2$ -18 and  $\text{TiO}_2$ -23 developed polyhedral particles

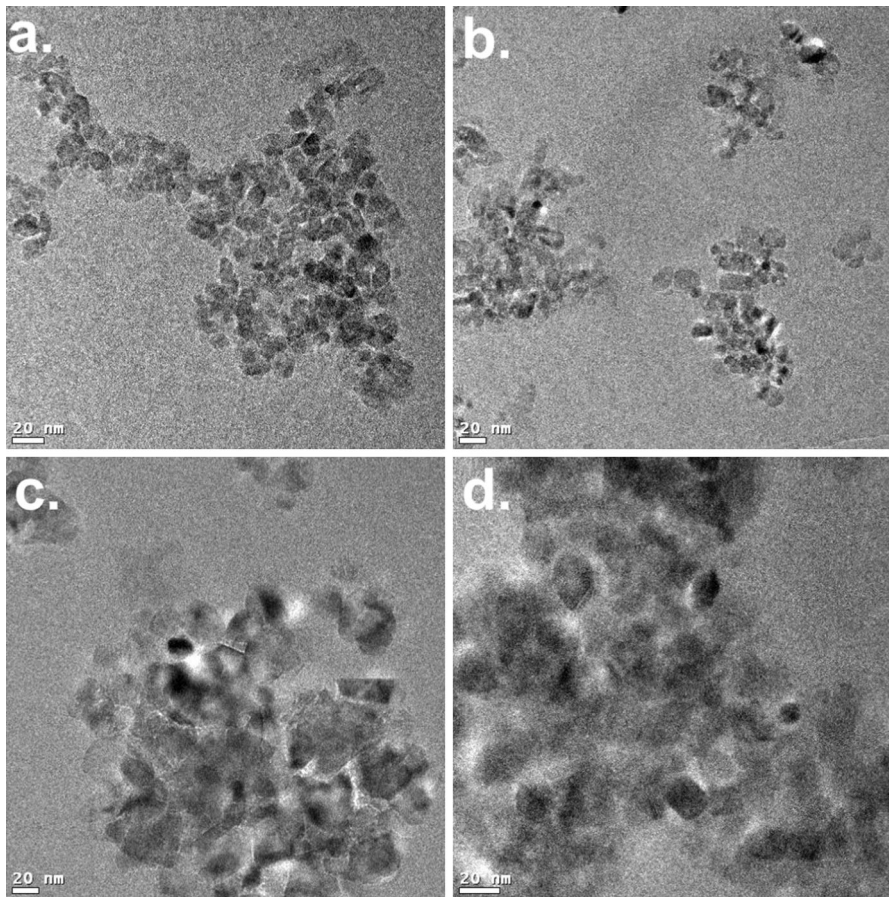


**Fig. 4** TEM images of some  $\text{TiO}_2$  representative samples prepared by the sol-gel method: **a**  $\text{TiO}_2$ -7, **b**  $\text{TiO}_2$ -27, **c**  $\text{TiO}_2$ -18, and **d**  $\text{TiO}_2$ -23

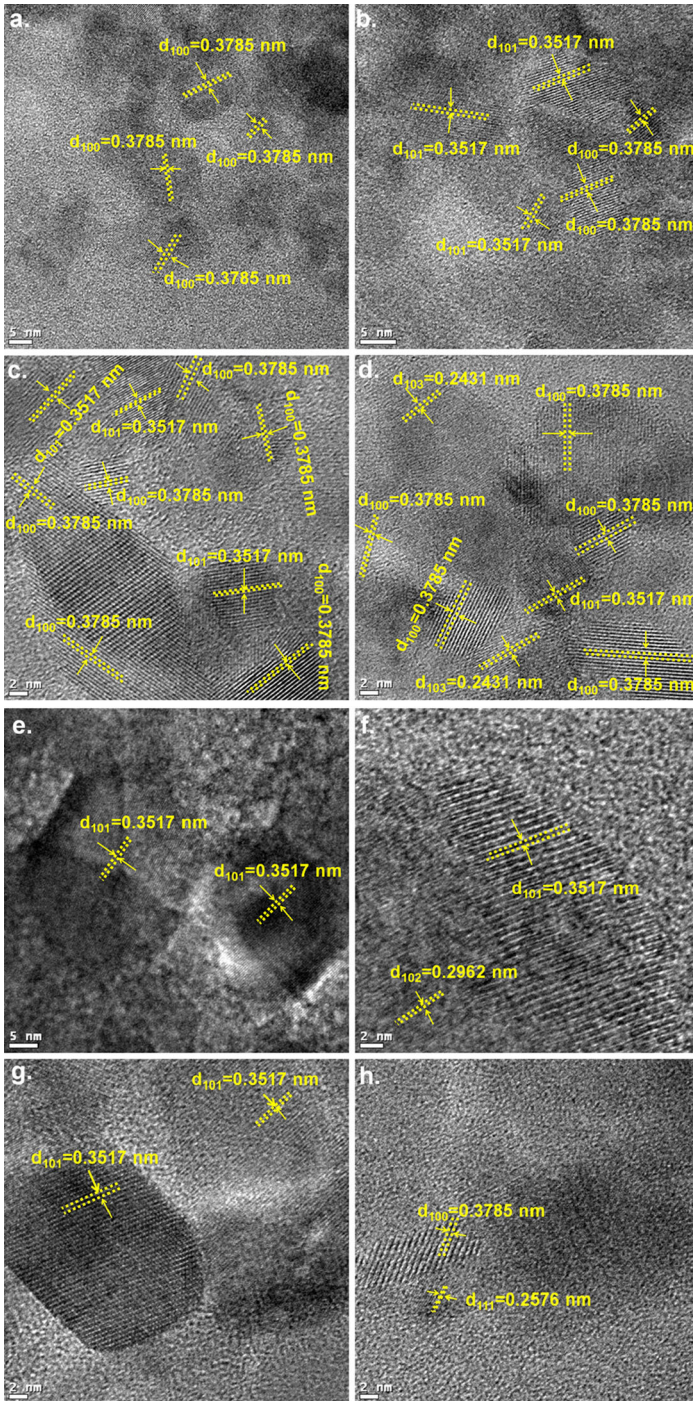
with an average size of 33 and 27 nm, respectively (Fig. 4c, d). Unlike the SEM analysis, the TEM technique provides a notable difference between the samples. Additionally, samples TiO<sub>2</sub>-18 and TiO<sub>2</sub>-23 showed an important agglomeration between its particles relative to the TiO<sub>2</sub>-7 and TiO<sub>2</sub>-27 samples, in which a greater dispersion of particles was observed.

In previous works, the photocatalytic activity of TiO<sub>2</sub> samples was associated with the preferential orientation of the crystals exposed to the reaction medium. According to the literature, the facets of the anatase polymorph with high photocatalytic activity are listed in the following order: (100) > (101) > (001). For this purpose, the four samples were analyzed at high resolution (HRTEM) to determine the interplanar distance and facets presents in the particles. The TEM images in Fig. 5a, d show that facet (100) was preferably present in the samples with the highest photocatalytic activity, i.e. TiO<sub>2</sub>-7 and TiO<sub>2</sub>-27. A representative detailed image in a second zone of these samples revealed the presence of the (101) facet although in a minor proportion. In contrast, the analysis carried out on the particles of samples with the lowest photocatalytic activity, TiO<sub>2</sub>-18 and TiO<sub>2</sub>-23, showed a preferential orientation in the (101) facet (Fig. 5e, h). In the X-ray powder diffraction, the (100) is a forbidden reflection and a comparison between the intensities associated with this plane for each sample analyzed was not possible. Nevertheless, a comparison of the profile of reflection associated with the (101) plane revealed a higher intensity in the samples with lowest photocatalytic activity, TiO<sub>2</sub>-18 and TiO<sub>2</sub>-23.

The above results are of considerable importance since the photocatalytic activity of TiO<sub>2</sub> samples can be influenced by the orientation of their crystals. Thus, TEM analysis introduces a differentiating element between the samples that can be used for establishing the origin of their different photocatalytic activities, beyond other physical properties of the material such as the surface area.

### Effect of the mass of photocatalyst in NO conversion degree

According to the experimental results, sample TiO<sub>2</sub>-7 was selected for subsequent experiments due to it having the highest degree of NO conversion (80 %) when was used as photocatalyst. Figure 6 shows the effect of modifying the mass of the photocatalyst in the degree of NO conversion using an exposure area of 0.08 m<sup>2</sup> under a UV irradiation average of 8.2 W m<sup>-2</sup>. A decrease of 99.3–87.9 % in the degree of NO conversion was observed when the mass of photocatalyst was reduced from 200 to 100 mg. A more remarkable effect was seen by decreasing the mass to 50 mg, at which 80 % of the degree of conversion was barely reached (Fig. 6a). For comparative purposes, additional experiments were performed using the commercial oxide TiO<sub>2</sub> (Degussa, P-25). It was noted that, although the degree of NO conversion was not affected by reducing the mass of the commercial photocatalyst from 200 to 100 mg, a notable decrease was observed when a mass of 50 mg was used (Fig. 6b). When both photocatalysts were tested under a condition of low mass per m<sup>2</sup>, i.e., 50 mg, it was observed that sample TiO<sub>2</sub>-7 had a minor deactivation, leading to the degree of NO conversion of 22 % higher than the value observed for TiO<sub>2</sub> P-25. Under this experimental condition, the specific surface area of the



◀ **Fig. 5** HRTEM images of some TiO<sub>2</sub> representative samples prepared by the sol-gel method: **a, b** TiO<sub>2</sub>-7, **c, d** TiO<sub>2</sub>-27, **e, f** TiO<sub>2</sub>-18, and **g, h** TiO<sub>2</sub>-23

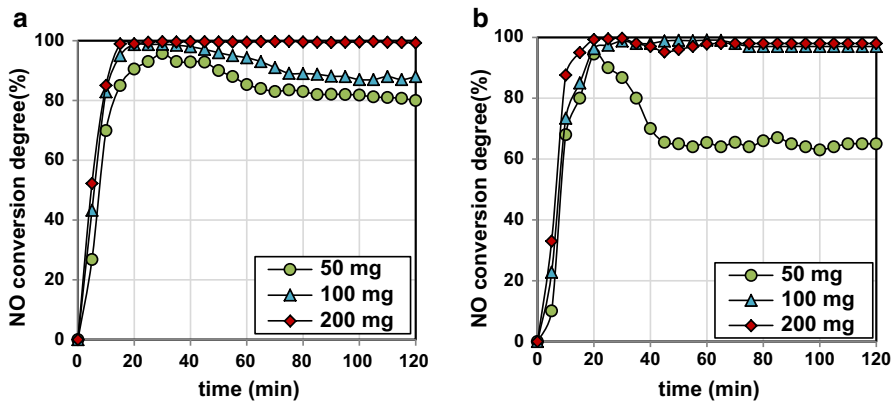


**Fig. 6** Evolution of the degree of NO conversion (%) by using different masses of the photocatalysts: **a** TiO<sub>2</sub>-7, **b** P-25 ( $Q = 1 \text{ L min}^{-1}$ ,  $I = 8.2 \text{ W m}^{-2}$ )

samples can be the main cause of differentiation in the photocatalytic activity between the two oxides, due to the importance of the adsorption phenomenon in experiments performed with low amount of mass. In this sense, TiO<sub>2</sub>-7 has double the specific surface area compared with that observed for TiO<sub>2</sub> P-25. The reduction of the mass of the photocatalyst is equivalent to observing its performance in more drastic operating conditions, helping to determine in a short time the material with the highest photocatalytic activity, especially considering the high activity of TiO<sub>2</sub>.

**Evaluation of the constants of velocity and adsorption**

The model of Langmuir–Hinshelwood is widely used in the literature to calculate the constant of velocity in the oxidation of gaseous pollutants [24–26]. The model considers that only the gas adsorbed can be oxidized, and therefore the rate of disappearance of NO is defined by Eq. (7):

$$r_{\text{NO}} = \frac{kK_d C}{1 + K_d C} \tag{7}$$

where  $k$  represents the reaction rate constant,  $K_d$  is the adsorption constant of NO and  $C$  corresponds to the NO concentration in the gas mixture at time  $t$ . The mass balance is represented by Eq. (8):

$$v \frac{dC}{dx} = -r_{\text{NO}} \tag{8}$$

where  $x$  is the length of the active area. Equation (8) can be integrated considering the equation model of the plug flow reactor and the result is shown in Eq. (9):

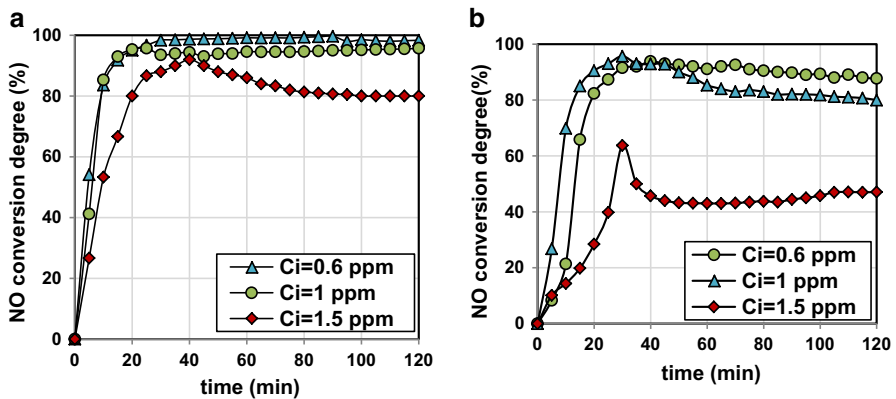


**Fig. 7** Evolution of the degree of NO conversion (%) by using  $\text{TiO}_2\text{-7}$  as a photocatalyst under different flow rates: **a**  $Q = 0.5 \text{ L min}^{-1}$ , **b**  $Q = 1 \text{ L min}^{-1}$  ( $m = 50 \text{ mg}$ ,  $I = 8.2 \text{ W m}^{-2}$ )

$$\frac{V}{Q(C_{\text{in}} - C_{\text{out}})} = \frac{1}{k} + \frac{1}{kK_d} \frac{\text{Ln}(C_{\text{in}} - C_{\text{out}})}{(C_{\text{in}} - C_{\text{out}})} \quad (9)$$

In order to calculate  $k$  and  $K_d$ , some experiments were performed modifying the volumetric flow ( $Q$ ) which entered the reactor ( $Q = 0.5$  and  $1.0 \text{ L min}^{-1}$ ) and the initial NO concentration ( $C_{\text{in}} = 600, 1000,$  and  $1500 \text{ ppb}$ ). The experiments were performed using a mass of  $50 \text{ mg}$  of  $\text{TiO}_2\text{-7}$  and the results are shown in Fig. 7. The degree of NO conversion decreased with increasing the initial concentration of gas because, for the same number of active sites of the photocatalyst, an increase in the concentration of NO molecules limits its conversion. In contrast, when the initial NO concentration was lower ( $600 \text{ ppb}$ ), the conversion degree reached values of  $87.7$  and  $98.4 \%$ , respectively when a flow rate of  $Q = 1$  and  $0.5 \text{ L min}^{-1}$  was used. The difference observed between the values of the degree of NO conversion can be associated with an increase in the residence time of the gas and, consequently, a higher interaction between the gas and reactive species generated during the photocatalytic process. Once the experiments were performed, Eq. (9) was plotted considering a line graph of the form of  $y = mx + b$ , where  $y = V/[Q(C_{\text{in}} - C_{\text{out}})]$  and  $x = \{\text{Ln}(C_{\text{in}} - C_{\text{out}})\}/(C_{\text{in}} - C_{\text{out}})$ . The generated equation was  $y = 15.89x + 38.42$ . The intersection of the straight line corresponded to  $1/k$ , and then the velocity constant was estimated as  $k = 0.02 \text{ mg m}^{-3} \text{ s}^{-1}$ . Also, the value of the adsorption constant,  $K_d$ , was calculated as  $2.4 \text{ m}^3 \text{ mg}^{-1}$ . According to previous works in gas phase photocatalysis, similar values of velocity and adsorption constant have been obtained. Nevertheless, a direct comparison is difficult due to the different conditions used in each work, such as volume of the reactor, inlet gas concentration, and the amount and type of irradiance.

### Effect of the irradiance and humidity on the constants of velocity and adsorption

Given that the photocatalytic reaction involves the absorption of radiation by the photocatalyst, some experiments were performed to investigate the effect of the

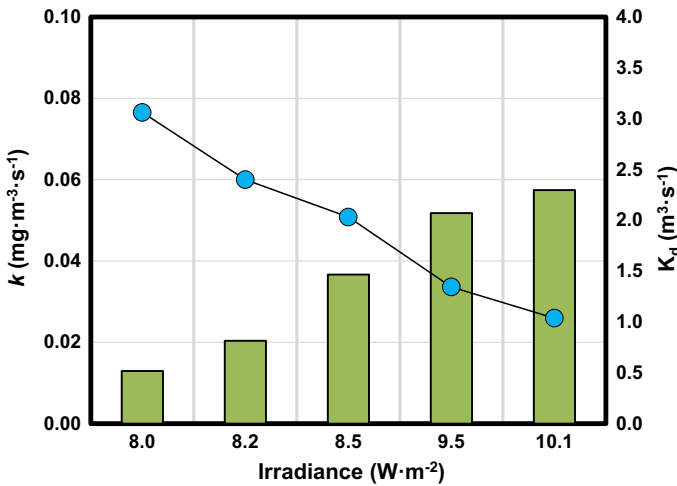


**Fig. 8** Effect of UV irradiance on the velocity and adsorption constants ( $Q = 1 \text{ L min}^{-1}$ )

irradiance in the degree of NO conversion. Figure 8 shows the obtained results for the constants of velocity and adsorption under different irradiances. The results showed a positive effect on the constant of velocity when the irradiance was increased. This is because increasing the irradiance in the reactor is feasible with more photocatalyst particles being activated by the irradiation. On the other hand, the adsorption constant showed a decrease in its value as the irradiance was increased. This fact can be associated with a hydrophilic effect developed on the surface of TiO<sub>2</sub> when it was illuminated by UV radiation. In previous works, this phenomenon has been demonstrated by contact angle measurements [27]. The contact angle ( $\theta$ ) decreased with increasing irradiance and irradiation time, reaching values of  $\theta$  close to  $0^\circ$ , indicating the development of a hydrophilic surface ( $\theta < 90^\circ$ ). The development of a hydrophilic surface directly affects the competition between the NO and H<sub>2</sub>O molecules for the adsorptive sites on the TiO<sub>2</sub> surface. However, this does not represent a direct reduction in the constant of velocity because, although the adsorption of NO molecules is diminished, there is now a higher amount of generated radical species by the effect of a higher irradiance. Considering that, during the photocatalytic reaction the NO molecules concentration considerably exceeds the reactive species generated by the photocatalyst, an increase in the value of  $k$  is expected due to a higher concentration of radicals, although a slight decrease in the value of  $K_d$  for NO molecules takes place.

Relative humidity (RH) is a factor that can influence the constant of velocity of a reaction carried out in the gaseous phase. Until this point, the experiments have been performed only in the presence of residual H<sub>2</sub>O vapor present in the synthetic air used as the carrier gas. Although this value is  $<0.4$  ppm, it is significant taking into account that it is of the same order as the initial concentration of NO in a typical experiment (1 ppm). Some experiments were performed in the reactor with the purpose to analyzing the effect of humidity on the constants of velocity and

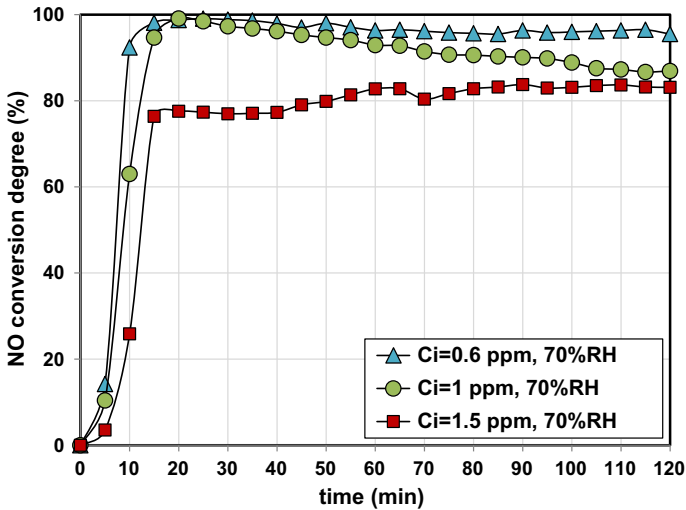


**Fig. 9** Evolution of degree of NO conversion (%) by using  $\text{TiO}_2\text{-7}$  as photocatalysts under 70 %RH ( $Q = 1 \text{ L min}^{-1}$ ,  $I = 8.2 \text{ W m}^{-2}$ )

adsorption. Figure 9 shows the evolution of the degree of NO conversion using  $\text{TiO}_2\text{-7}$  as photocatalyst in an experiment with 70 %RH. In the first minutes, the conversion is faster due to the presence of a higher concentration of  $\text{H}_2\text{O}$  molecules in the active sites of the photocatalyst, which promotes the photo-oxidation reaction of NO. This phenomenon is associated with the hydrophilic surface developed in the  $\text{TiO}_2$ . The formation of mono- and multilayers of  $\text{H}_2\text{O}$  molecules over the  $\text{TiO}_2$  surface takes place by contact of the  $\text{H}_2\text{O}$  vapor with the photocatalyst and contributes to producing (OH) radicals involved in the oxidation reaction of the pollutant [28]. Under these conditions, the degree of NO conversion reached values of 95, 87, and 83 % when the initial NO concentrations were 600, 1000, and 1500 ppb, respectively. According to these results,  $\text{H}_2\text{O}$  molecules seem to contribute by the generation of hydroxyl radicals increasing the efficiency of the reaction. This is reflected in the comparison with the values of the degree of NO conversion reached when the experiments were performed with  $<0.4 \text{ ppm H}_2\text{O}$ .

The irradiance in the reactor was increased to  $10.1 \text{ W m}^{-2}$  to observe the hydrophilic behavior of the  $\text{TiO}_2$  surface in the presence of humidity (Fig. 10). The degree of NO conversion was significantly higher in the presence of humidity under high irradiance values in comparison with the experiments performed with a lower humidity. Also, the presence of 70 %RH in the reactor increased the constant velocity by 20 % when the photocatalyst was irradiated with  $10.1 \text{ W m}^{-2}$  (Fig. 11a). With regard to the NO adsorption constant, it decreased by 36 % under these experimental conditions (Fig. 11b). The observed decrease in the adsorption constant with the increase of irradiance and humidity is in agreement with reports in the literature [29, 30]. This decrease can be explained on the basis of a higher affinity of the  $\text{H}_2\text{O}$  molecules to be adsorbed on the  $\text{TiO}_2$  surface due to its hydrophilic property. The adsorption of water molecules on the  $\text{TiO}_2$  surface implies a decrease



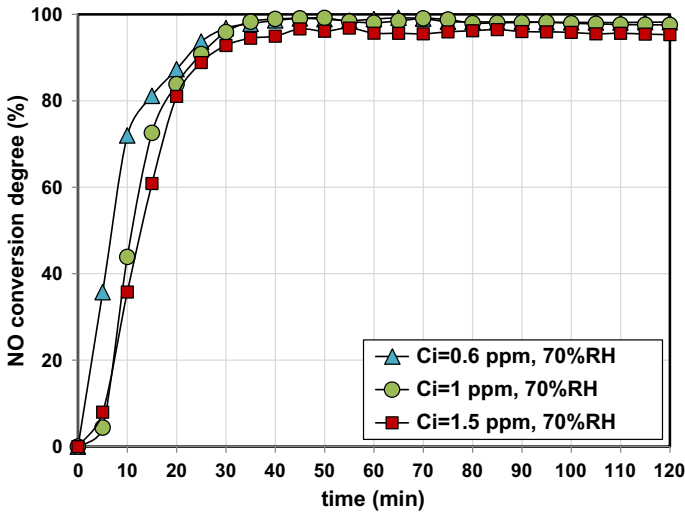


**Fig. 10** Evolution of the degree NO conversion (%) by using TiO<sub>2</sub>-7 as photocatalyst under 70 %RH. ( $Q = 1 \text{ L min}^{-1}$ ,  $I = 10.1 \text{ W m}^{-2}$ )

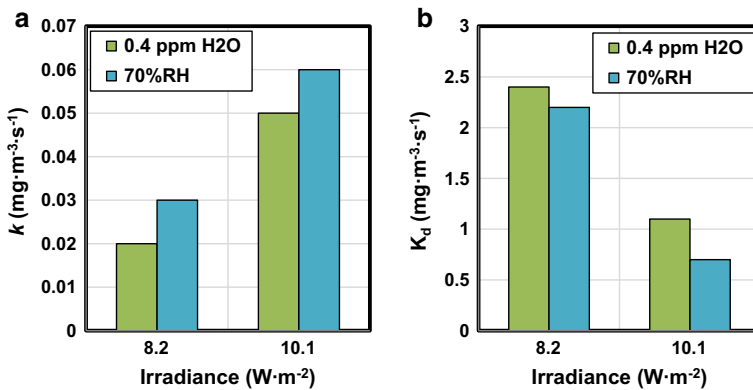
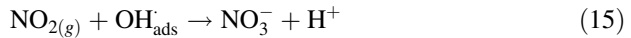
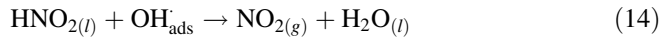
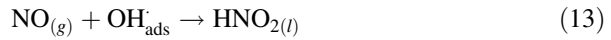
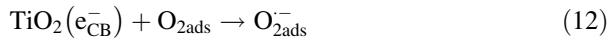
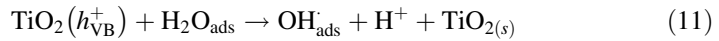


**Fig. 11** Effect of UV irradiance and humidity on the velocity and adsorption constants ( $Q = 1 \text{ L min}^{-1}$ )

in the contact angle as is expected for a hydrophilic surface. Therefore, the obtained results confirm that the TiO<sub>2</sub> surface develops a higher hydrophilic character in the presence of a higher irradiance and high RH. Also, the photocatalyst deactivation was inhibited under these conditions by the generation of a higher concentration of OH<sup>-</sup> radicals, even when the initial NO concentration was 1500 ppb.

**Analysis of reaction products**

The mechanism of the deep oxidation of NO by heterogeneous photocatalysis has been proposed previously and is described by Eqs. (10–16).



According to Eqs. (15) and (16), the nitrate ions are the main product of the deep NO photo-oxidation. The nitrate formation has been quantified in some representative photocatalytic experiments (see Table 3). Due to the synthesis route, the presence of nitrates or nitrites as by-products of the reaction in the TiO<sub>2</sub> samples is evident. In order to avoid interferences in the results, the samples used as photocatalysts were previously washed successively with deionized water, registering in each wash the amount of nitrate and nitrites extracted from the sample. This procedure was repeated until the accumulative mass of the ions was constant, which took place after 10 washes. Then, the washed sample was used as a photocatalyst in the NO photo-oxidation reaction for 2 h. After the photocatalytic reaction, the photocatalyst was washed in order to analyze the nitrate and nitrite ions associated with the NO oxidation reaction. As shown in Fig. 12, the accumulated mass of nitrate and nitrite ions increased after the photocatalytic reaction as a consequence of the formation of oxidation products of the NO molecules. Under the following experimental conditions:  $Q = 1 \text{ L min}^{-1}$ ,  $I = 8.2 \text{ W m}^{-2}$ , and  $C_i = 1 \text{ ppm}$ , the conversion of NO to NO<sub>3</sub><sup>-</sup> and NO<sub>2</sub><sup>-</sup> ions was 41 and 0.4 %, respectively.

The degree of conversion of NO to NO<sub>3</sub><sup>-</sup> and NO<sub>2</sub><sup>-</sup> ions was also investigated under different experimental conditions. By increasing the irradiance in the system,

**Table 3** Degree of NO conversion (%) and selectivity to NO<sub>3</sub><sup>-</sup>/NO<sub>2</sub><sup>-</sup> ions under different experimental conditions

Experimental conditions	Degree of NO conversion (%)	Conversion NO → NO <sub>3</sub> <sup>-</sup> (%)	Conversion NO → NO <sub>2</sub> <sup>-</sup> (%)
1 ppm; 1 L min <sup>-1</sup> ; 8.2 W m <sup>-2</sup> ; < 0.4 ppm H <sub>2</sub> O	82.0	41.2	0.40
1 ppm; 1 L min <sup>-1</sup> ; 8.5 W m <sup>-2</sup> ; < 0.4 ppm H <sub>2</sub> O	85.9	49.9	0.41
1 ppm; 1 L min <sup>-1</sup> ; 10.1 W m <sup>-2</sup> ; < 0.4 ppm H <sub>2</sub> O	95.4	77.3	2.85
1 ppm; 1 L min <sup>-1</sup> ; 8.2 W m <sup>-2</sup> ; 70 %RH	91.3	85.0	0.70

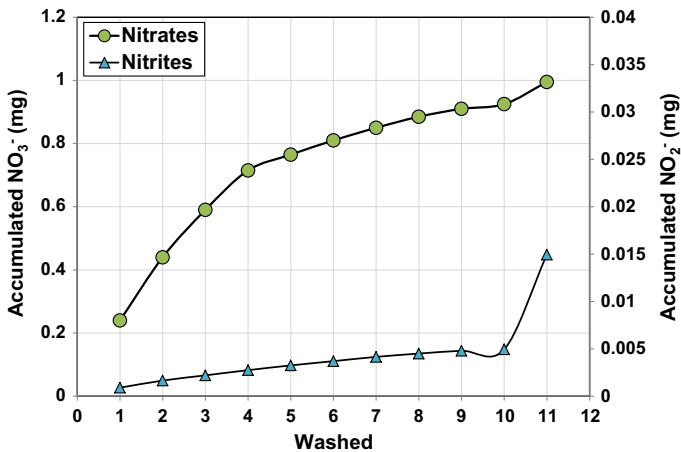


**Fig. 12** Accumulated mass of reaction products (NO<sub>3</sub><sup>-</sup>, NO<sub>2</sub><sup>-</sup>) using TiO<sub>2</sub>-7 as photocatalyst ( $I = 8.2 \text{ W m}^{-2}$ ,  $Q = 1 \text{ L min}^{-1}$ ,  $C_i = 1 \text{ ppm}$ , 70 %RH)

the selectivity of the conversion of NO to NO<sub>3</sub><sup>-</sup> ions was increased up to 77 % for an irradiance value of 10.1 W m<sup>-2</sup> (Table 3). Concerning the formation of nitrite ions, the highest value was obtained in the experiment performed with the highest irradiance, in which a conversion of NO to NO<sub>2</sub><sup>-</sup> of 3 % was reached.

In the same way, an experiment was performed in the presence of higher humidity. The results of the quantification of the ions revealed that, under these experimental conditions, the NO conversion to innocuous products was higher compared with the previous experiments, reaching a conversion of NO to NO<sub>3</sub><sup>-</sup> ions of 85 %. Furthermore, the formation of nitrite ions was low (<0.7 % of NO to NO<sub>2</sub><sup>-</sup>), indicating the ability of the photocatalyst to conduct a complete oxidation of NO under a high value of humidity.

## Conclusions

TiO<sub>2</sub> samples were prepared successfully by the sol–gel method applying a factorial design of the type 3<sup>*n*</sup> ( $n = 3$ ). As a direct consequence of modifying three experimental variables of synthesis, the physical properties of TiO<sub>2</sub> samples were strongly influenced and led to the formation of samples with different photocatalytic activity. In particular, the calcination temperature played the most important role to obtain materials with high photocatalytic activity for the photo-oxidation reaction of NO gas. Although a good correlation was observed between the values of the degree of NO conversion predicted by the mathematical model and that obtained experimentally, some differences were observed. This situation was associated with some physical properties not considered in the mathematical model, e.g., the dispersion of the photocatalyst on the substrate. Additionally, the preferential orientation of the exposed crystals seems to play an important role in the degree of NO conversion reached by each TiO<sub>2</sub> sample.

The effects on the photocatalytic reaction of the mass of the photocatalyst, the flow rate, the irradiance in the reactor and the humidity were also investigated. The constants of velocity and adsorption were evaluated and their values were associated with the different operating conditions in the photocatalytic reactor. The presence of reaction products was successfully confirmed. In general, an increase in the humidity and irradiance had a positive effect on the selective oxidation of NO to NO<sub>3</sub><sup>-</sup> ions. According to the results, it was confirmed that NO<sub>3</sub><sup>-</sup> ions were the main product of the NO photo-oxidation reaction.

**Acknowledgment** We wish to thank to the CONACYT for its invaluable support through the Project 167018.

## References

1. J.Z. Bloh, A. Follia, D.E. Macphee, RSC Adv. **4**, 45726–45734 (2014)
2. J. Ângelo, L. Andrade, L.M. Madeira, A. Mendes, J. Environ. Manag. **129**, 522–539 (2013)
3. J. Lasek, Y. Yu, J.C.S. Wu, J. Photochem. Photobiol., C **14**, 29–52 (2013)
4. S.W. Verbruggen, J. Photochem. Photobiol. C Photochem. Rev. **24**, 64–82 (2015)
5. A. Fritz, V. Pitchon, Appl. Catal. B **13**, 1–25 (1997)
6. Q.L. Yu, H.J.H. Brouwers, Appl. Catal. B **99**, 58–65 (2010)
7. Y. Hu, X. Song, S. Jiang, C. Wei, Chem. Eng. J. **274**, 102–112 (2015)
8. D. Xia, L. Hu, C. He, W. Pan, T. Yang, Y. Yang, D. Shu, Chem. Eng. J. **279**, 929–938 (2015)
9. F. Dong, Z. Zhao, Y. Sun, Y. Zhang, S. Yan, Z. Wu, Environ. Sci. Technol. **49**, 12432–12440 (2015)
10. Z. Zhao, Y. Sun, Q. Luo, F. Dong, H. Li, W.K. Ho, Scientific Reports 5, Article number: 14643 (2015)
11. R. Amadelli, L. Samiolo, M. Borsa, M. Bellardita, L. Palmisano, Catal. Today **206**, 19–25 (2013)
12. C. Huang, I. Wang, Y. Lin, Y. Tseng, C. Lu, J. Mol. Catal. A: Chem. **316**, 163–170 (2010)
13. S. Devahasdin, C. Fan, J.K. Li, D.H. Chen, J. Photochem. Photobiol. A **156**, 161–170 (2003)
14. F.L. Toma, G. Bertrand, D. Klein, C. Coddet, Environ. Chem. Lett. **2**, 117–121 (2004)
15. T. Ibusuki, K. Takeuchi, J. Mol. Catal. **88**, 93–102 (1994)
16. C.H. Ao, S.C. Lee, J. Photochem. Photobiol., A **161**, 131–140 (2004)
17. B.N. Shelimov, N.N. Tolkachev, O.P. Tkachenko, G.N. Baeva, K.V. Klementiev, A.Y. Stakheev, V.B. Kazansky, J. Photochem. Photobiol., A **195**, 81–88 (2008)
18. M. Aparicio, A. Itianu, L.C. Klein, *Sol-Gel Processing for Conventional and Alternative Energy* (Springer, New York, 2012), pp. 217–230
19. M.C. Hidalgo, M. Aguilar, M. Maicu, J.A. Navío, G. Colón, Catal. Today **129**, 50–58 (2007)
20. S. Valencia, J.M. Marín, G. Restrepo, Open Mater. Sci. J. **4**, 9–14 (2010)
21. M.A. Santana-Aranda, M. Morán-Pineda, J. Hernández, S. Castillo, Superf. Vacío **18**, 46–49 (2005)
22. J.B. Condon, *Surface Area and Porosity Determinations by Physisorption* (Elsevier, Amsterdam, 2006), pp. 8–9
23. L.L. Hench, J.K. West, Chem. Rev. **90**, 33–72 (1990)
24. L. Yang, Z. Liu, J. Shi, H. Hu, W. Shangguan, Catal. Today **126**, 359–368 (2007)
25. Y. Ku, C. Ma, Y. Shen, Appl. Catal. B **34**, 181–190 (2001)
26. A.A. Assadi, A. Bouzaza, S. Merabet, D. Wolbert, Chem. Eng. J. **258**, 119–127 (2014)
27. N. Sakai, A. Fujishima, T. Watanabe, K. Hashimoto, J. Phys. Chem. B **107**, 1028–1035 (2003)
28. H. Dylla, M.M. Hassan, L.J. Thibodeaux, Transp. Res. Board Annu. Meet. **93**, 1–17 (2014)
29. S. Broillon, L. Lhomme, C. Vallet, A. Bouzaza, D. Wolbert, Appl. Catal. B **78**, 232–241 (2008)
30. P. Zhang, J. Liu, J. Photochem. Photobiol., A **167**, 87–94 (2004)